Supporting Information

Anionic Europium (III) Coordination Polymer for Highly Selective and Sensitive Detection of Fe^{3+} and 4-Nitrophenol

Raji Feyisa Bogale, Junwei Ye,* Yuan Sun, Tongxin Sun, Siqi Zhang, Abdul Rauf, Cheng Hang, Peng Tian, Guiling Ning*

State Key Laboratory of Fine Chemicals and School of Chemical Engineering, Faculty of Chemical, Environmental and Biological Science and Technology, Dalian University of Technology, Linggong Road, Dalian 116024, P. R. China

E-mail: junweiye@dlut.edu.cn; ninggl@dlut.edu.cn; Fax: +86-041184986065; Tel: +86-0411-84986067

Figure Captions

Fig. S1 View of 2D packing network (a) and hydrogen bonds (b) in **1**.

Fig. S2 The photoluminescence spectrum of **1** at solid state.

Fig. S3. Comparison of the luminescence intensity of **1** interacting with different metal ions under the same conditions.

Fig. S4. Comparison of the luminescence intensity of **1** interacting with different anions in aqueous solution under the same conditions.

Fig. S5. Photoluminescence intensity of the $^5D_0 \rightarrow {}^7F_2$ transition (615 nm) of **1** treated with 1 mM different nitrocompounds under the same conditions.

Fig. S6 Comparison of the luminescence intensity exited at 290 nm of 1 (0.02 mg dispersed in 3ml of ethanol) interacting with phenol and 4-Bromophenol (1 mM in ethanol) under the same conditions.

Fig. S7 Comparison of the luminescence intensity exited at 290 nm (a) and UV-Vis absorption spectra (b) of 1 (0.02 mg dispersed in 3ml ethanol) interacting with 160 μL Fe^{3+} (10 mM), 240 μL 4-NP (1 mM), and both mixed Fe^{3+} + 4-NP (1:1) under the same conditions

Fig. S8 Photoluminescence emission spectra exited at 290 nm of **1** dispersed in the ethanol upon volume incremental addition of a) Zn^{2+} b) Mg^{2+} c) TNP d) 2,6-DNT

Fig. S9 Thermogravimetric analysis of **1** before and after immersion in Fe^{3+}-containing aqueous solution

Fig. S10. Comparison of EDX measurements and SEM images of **1** (a, c) and Fe@**1** (b, d).

Fig. S11 Absorption spectra of **1** dispersed in the ethanol and after 240 μL Fe^{3+} aqueous solution was added to the dispersed solution.

Fig. S12 Fluorescence lifetime curves of **1** in the presence and absence of both $Fe^{3+}$and 4-NP analytes respectively.

Fig. S13 UV-Vis absorption spectra of **1** dispersed in ethanol treated with different nitrocompounds.

Table Captions

Table S1. Crystal data and structure refinement for **1.**

Table S2. Selected bond lengths and angles of **1.**

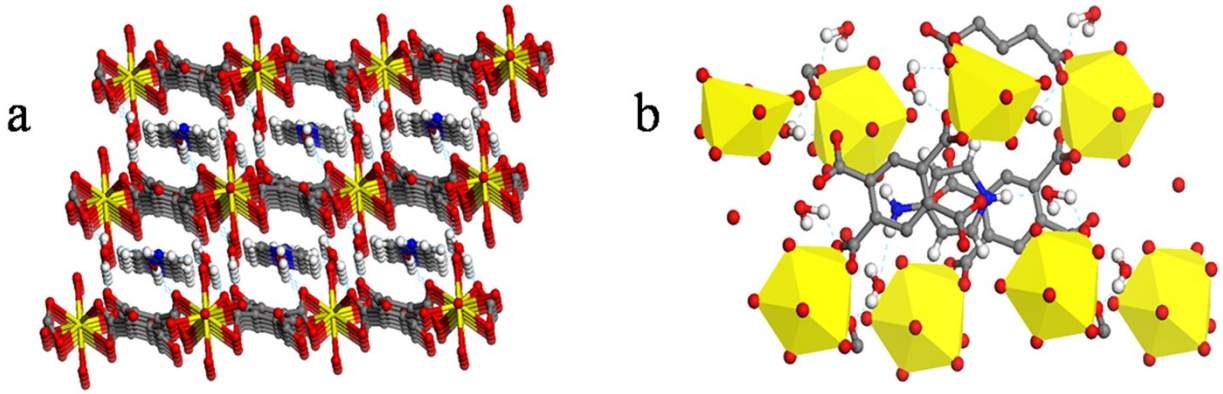

Fig. S1 View of 2D packing network (a) and hydrogen bonds (b) in **1**.

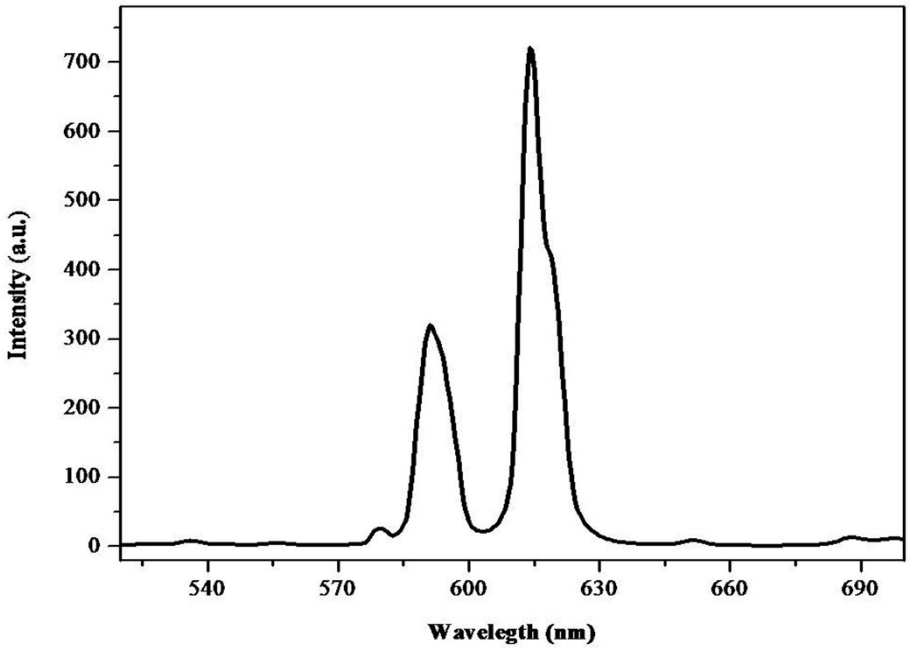

Fig. S2 The photoluminescence spectrum of **1** at solid state.

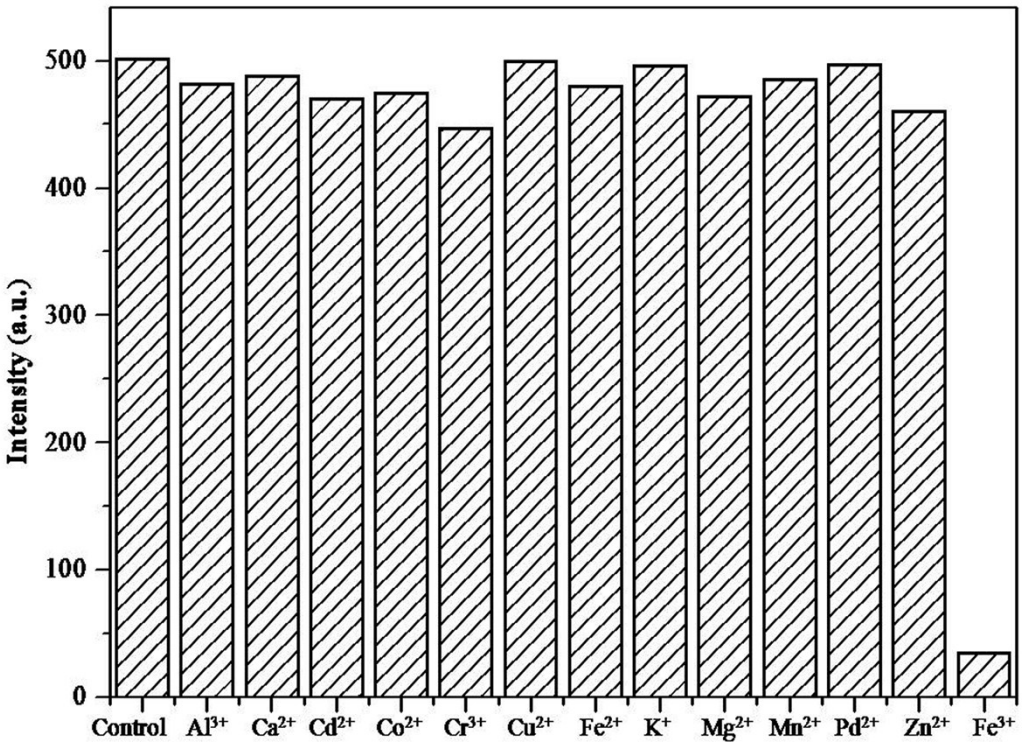

Fig. S3 Comparison of the luminescence intensity exited at 290 nm of **1** (0.02 mg in ethanol) after interacting with equal volume of 160 μL different metal ions (10 mM in water) under the same conditions.

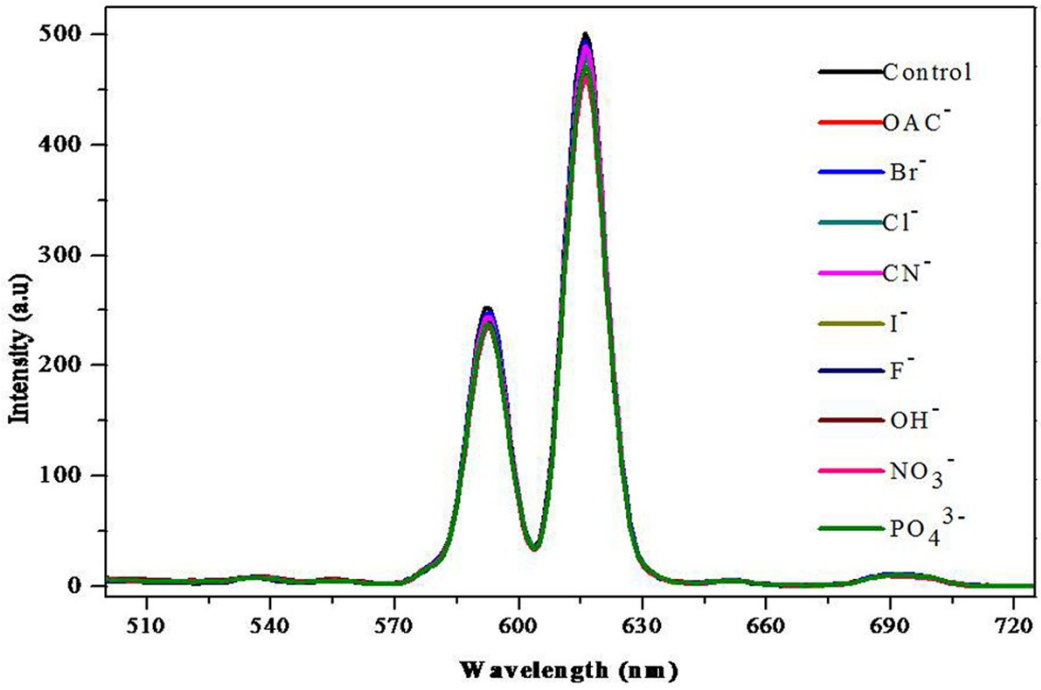

Fig. S4 Comparison of the luminescence intensity exited at 290 nm of **1** (0.02 mg dispersed in 3ml of ethanol) interacting with different anions (10 mM in water) under the same conditions.

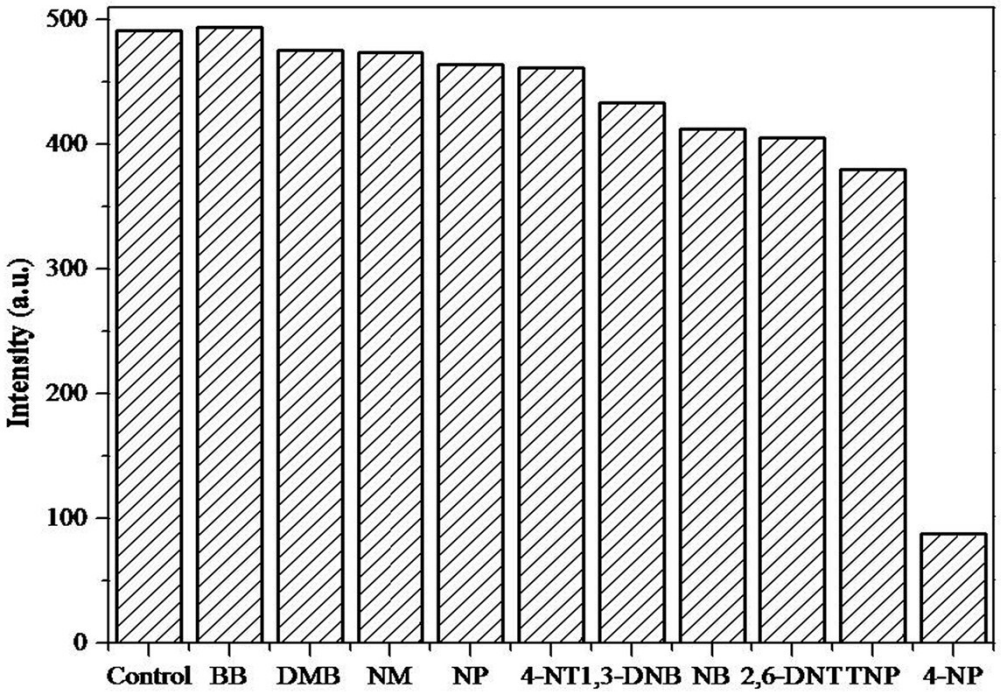

Fig. S5 Photoluminescence intensity exited at 290 nm of the $^5D_0 \rightarrow {}^7F_2$ transition (615 nm) of **1** (0.02 mg in 3 mL ethanol) after treated with equal volume of 240 μL different nitrocompounds solution (1 mM in water) under the same conditions.

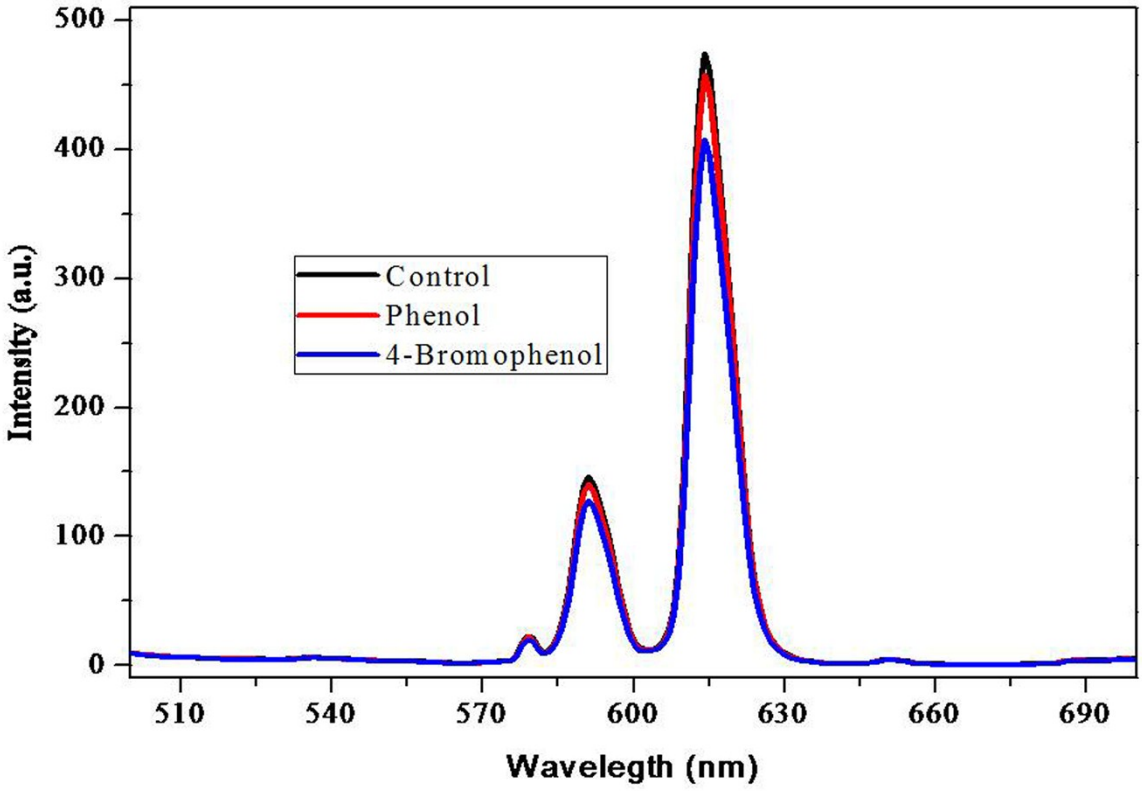

Fig. S6 Comparison of the luminescence intensity exited at 290 nm of **1** (0.02 mg dispersed in 3ml of ethanol) interacting with 240 μL of phenol and 4-bromophenol (1 mM in ethanol) under the same conditions.

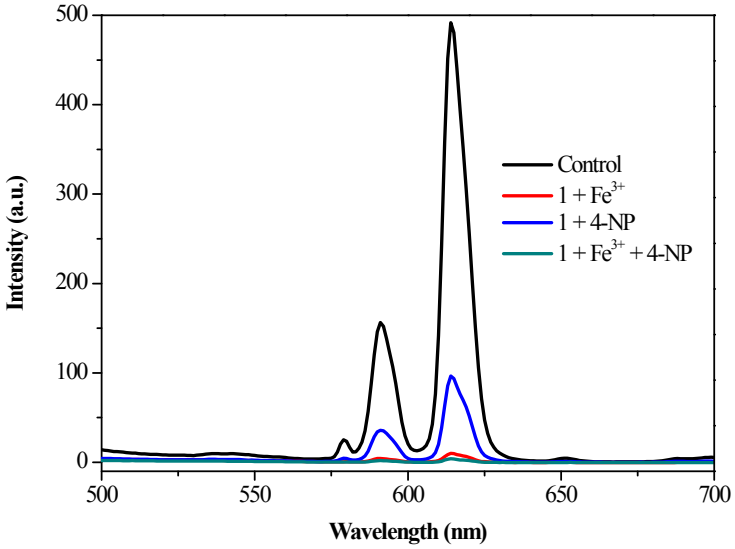

Fig. S7 Comparison of the luminescence intensity exited at 290 nm of **1** (0.02 mg dispersed in 3mL ethanol) interacting with 160 μL Fe^{3+} (10 mM), 240 μL 4-NP (1 mM), and both mixed Fe^{3+} + 4-NP (1:1) under the same conditions.

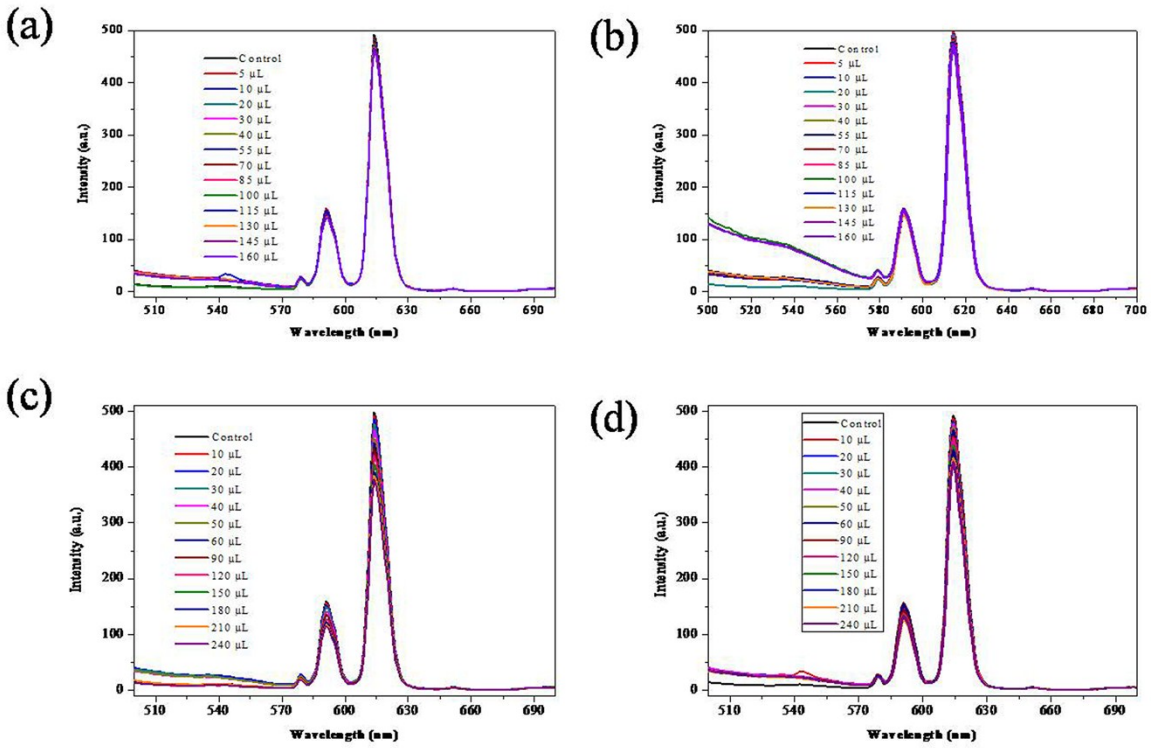

Fig. S8 Photoluminescence emission spectra exited at 290 nm of **1** (0.02 mg dispersed in the ethanol) upon volume incremental addition of a) Zn^{2+} (10 mM in water) b) Mg^{2+} (10 mM in water) c) TNP (1 mM in ethanol) d) 2,6-DNT (1 mM in ethanol)

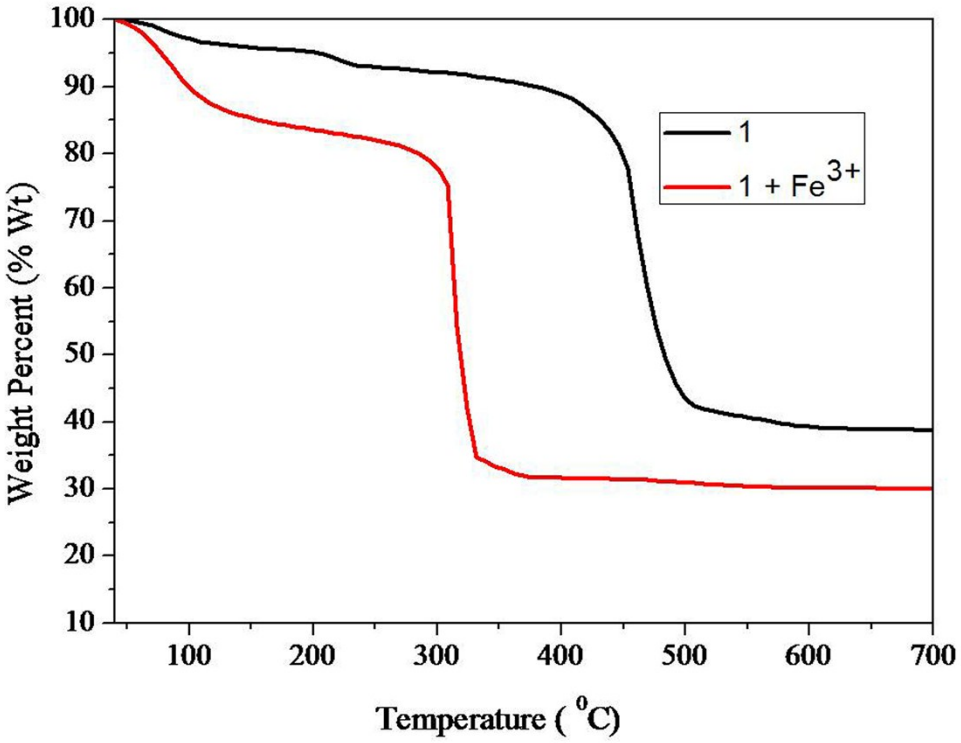

Fig. S9 Thermogravimetric analysis of **1** before and after immersion in Fe^{3+}-containing aqueous solution

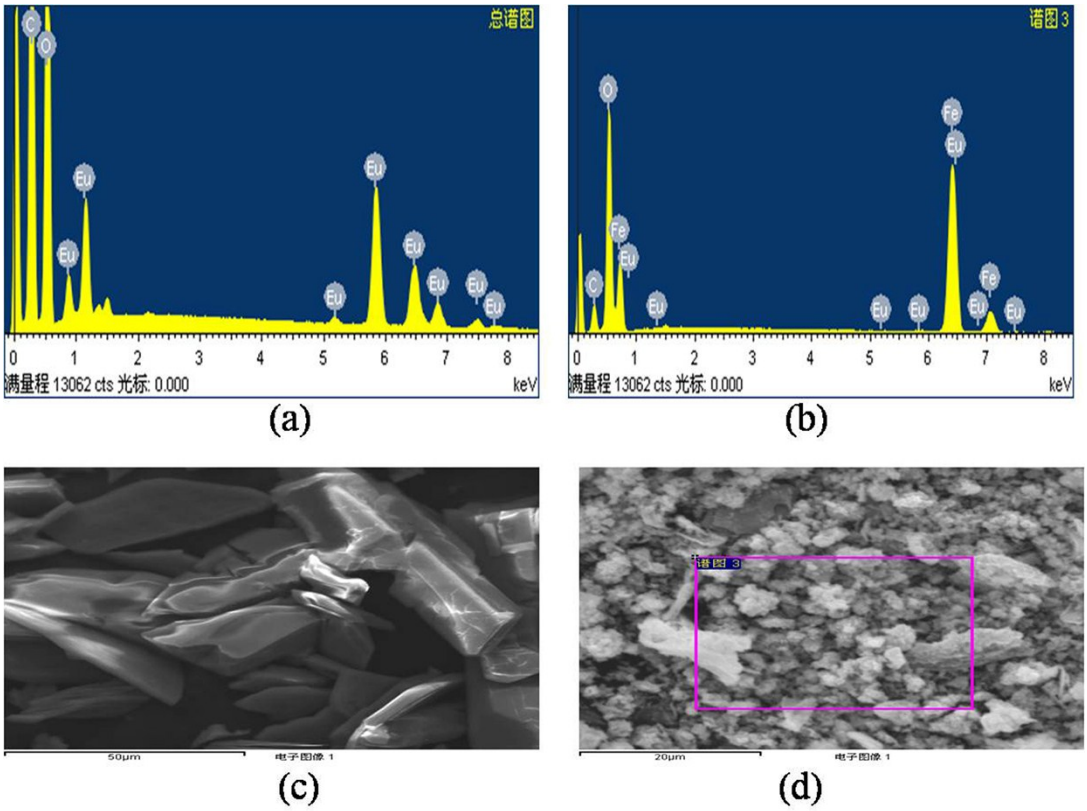

Fig. S10 Comparison of EDX measurements and SEM images of **1** (a, c) and Fe@**1** (b, d).

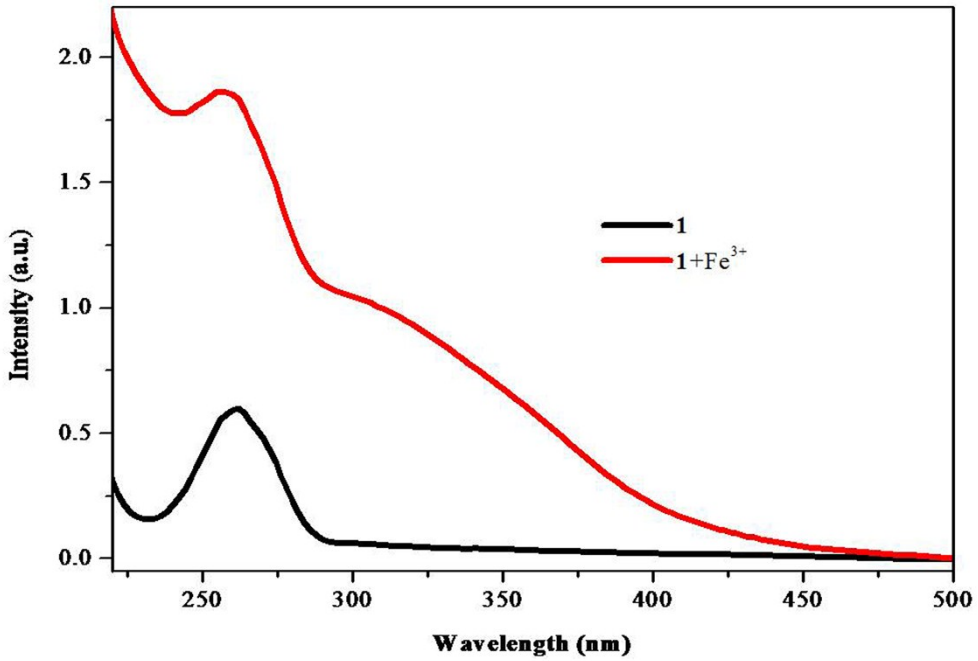

Fig. S11 Absorption spectra of **1** dispersed in the ethanol and after 240 μL Fe^{3+} aqueous solution (10 mM) was added to the dispersed solution of **1** (0.02 mg in ethanol)

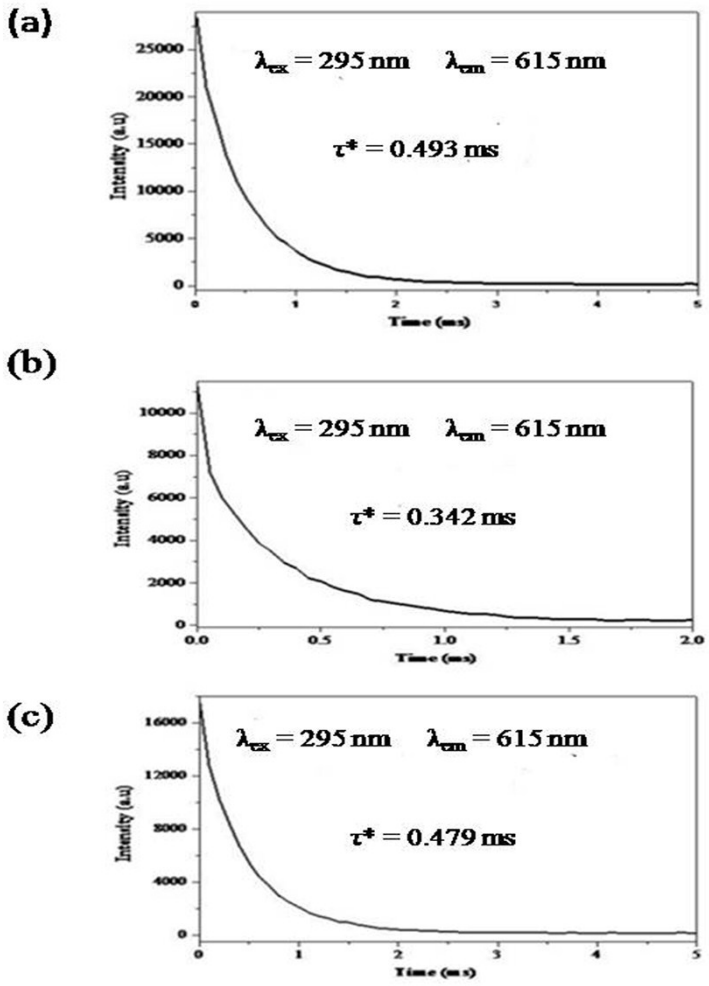

Fig. S12 Fluorescence lifetime curves of **1** dispersed in ethanol (a), after treated with Fe^{3+} aqueous solution (160 μL) (b), and after treated with 4-NP (240 μL) (c).

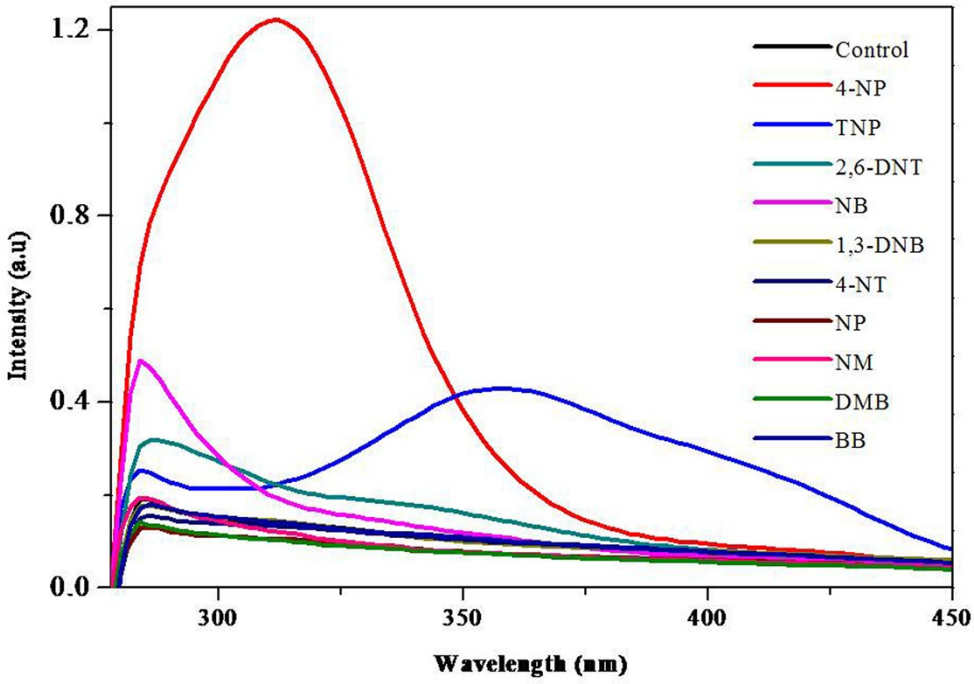

Fig. S13 UV-Vis absorption spectra of **1** (0.96 mg dispersed in 3 mL ethanol) treated with different nitrocompounds having equal volumes (240 μL) and concentration of 1 mM in ethanol for each

Table S1 Crystal data and structure refinement for **1.**

Empirical formula	$C_{15}H_{25}EuN_2O_{16}$
Formula weight	641.33
Crystal system	Monoclinic, C2/c
a (Å)	13.0689(8)
b (Å)	11.2535(6)
c (Å)	15.4306(9)
α(º)	90
β (º)	105.9080(10)
γ(º)	90
Volume (Å^3)	2182.5(2)
Z	4
D_{Calc}（mg/m^{-3}）	1.952
μ (mm^{-1})	2.959
$F_{(000)}$	1280
R_{int}	0.0248
GOF on F^2	1.087
R_1 [$I>2\sigma(I)$]*	0.0218
wR_2 [$I>2\sigma(I)$]*	0.0522
R_1 (all data) *	0.0233
wR_2 (all data)*	0.0532

*$R_1 = \Sigma||F_o|-|F_c||/\Sigma|F_o|$; $wR_2 = \{\Sigma[w(F_o^2-F_c^2)^2]/\Sigma[w(F_o^2)]^2\}^{1/2}$

Table S2 Selected bond lengths [Å] and angles [deg] for **1.**

Eu(1)-O(5)	2.4039(17)	Eu(1)-O(2)$^{\#1}$	2.4596(16)
Eu(1)-O(5)$^{\#1}$	2.4039(17)	Eu(1)-O(7)	2.496(2)
Eu(1)-O(6)$^{\#1}$	2.4282(19)	Eu(1)-O(1)$^{\#1}$	2.5550(16)
Eu(1)-O(6)	2.4282(19)	Eu(1)-O(1)	2.5550(16)
Eu(1)-O(2)	2.4596(16)		
O(5)-Eu(1)-O(5)$^{\#1}$	136.88(8)	O(6)$^{\#1}$-Eu(1)-O(7)	79.36(5)
O(5)-Eu(1)-O(6)$^{\#1}$	93.48(7)	O(6)-Eu(1)-O(7)	79.36(5)
O(5)$^{\#1}$-Eu(1)-O(6)$^{\#1}$	78.68(7)	O(2)-Eu(1)-O(7)	141.20(4)
O(5)-Eu(1)-O(6)	78.68(7)	O(2)$^{\#1}$-Eu(1)-O(7)	141.20(4)
O(5)$^{\#1}$-Eu(1)-O(6)	93.48(7)	O(5)-Eu(1)-O(1)$^{\#1}$	140.40(6)
O(6)$^{\#1}$-Eu(1)-O(6)	158.72(9)	O(5)$^{\#1}$-Eu(1)-O(1)$^{\#1}$	69.65(6)
O(5)-Eu(1)-O(2)	76.74(6)	O(6)$^{\#1}$-Eu(1)-O(1)$^{\#1}$	124.26(6)
O(5)$^{\#1}$-Eu(1)-O(2)	143.34(6)	O(6)-Eu(1)-O(1)$^{\#1}$	69.48(6)
O(6)$^{\#1}$-Eu(1)-O(2)	120.28(6)	O(2)-Eu(1)-O(1)$^{\#1}$	73.94(5)
O(6)-Eu(1)-O(2)	77.50(6)	O(2)$^{\#1}$-Eu(1)-O(1)$^{\#1}$	51.69(5)
O(5)-Eu(1)-O(2)$^{\#1}$	143.34(6)	O(7)-Eu(1)-O(1)$^{\#1}$	125.11(4)
O(5)$^{\#1}$-Eu(1)-O(2)$^{\#1}$	76.74(6)	O(5)-Eu(1)-O(1)	69.65(6)
O(6)$^{\#1}$-Eu(1)-O(2)$^{\#1}$	77.50(6)	O(5)$^{\#1}$-Eu(1)-O(1)	140.40(6)
O(6)-Eu(1)-O(2)$^{\#1}$	120.28(6)	O(6)$^{\#1}$-Eu(1)-O(1)	69.48(6)
O(2)-Eu(1)-O(2)$^{\#1}$	77.60(8)	O(6)-Eu(1)-O(1)	124.26(6)
O(5)-Eu(1)-O(7)	68.44(4)	O(2)-Eu(1)-O(1)	51.69(5)
O(5)$^{\#1}$-Eu(1)-O(7)	68.44(4)	O(2)$^{\#1}$-Eu(1)-O(1)	73.94(5)
O(1)$^{\#1}$-Eu(1)-O(1)	109.78(7)	O(7)-Eu(1)-O(1)	125.11(4)

Symmetry transformations used to generate equivalent atoms: #1 -x,y,-z+1/2